Published in final edited form as:
*J Cell Sci*. 2007 December 15; 120(Pt 24): 4278–4288. doi:10.1242/jcs.014217.

# Myosin VI and its interacting protein LMTK2 regulate tubule formation and transport to the endocytic recycling compartment

**Margarita V. Chibalina**[*], **Matthew N.J. Seaman**[*], **Christopher C. Miller**[‡], **John Kendrick-Jones**[¶], and **Folma Buss**[*]

[*]Cambridge Institute for Medical Research, University of Cambridge, Wellcome Trust/MRC Building, Hills Road, Cambridge CB2 2XY, UK

[‡]Departments of Neuroscience and Neurology, The Institute of Psychiatry, Kings College London, London SE5 8AF, UK

[¶]MRC Laboratory of Molecular Biology, Hills Road, Cambridge CB2 2QH, UK

## Summary

Myosin VI is an actin-based retrograde motor protein, which plays a crucial role in both endocytic and secretory membrane trafficking pathways. Myosin VI's targeting to and function in these intracellular pathways is mediated by a number of specific binding partners. In this paper we have identified a new myosin VI binding partner, Lemur tyrosine kinase 2 (LMTK2), which is the first transmembrane protein and kinase that directly binds to myosin VI. LMTK2 binds to the WWY site in the C-terminal myosin VI tail, the same site as the endocytic adaptor protein Dab2. When either myosin VI or LMTK2 is depleted by siRNA, the transferrin receptor (TfR) is trapped in swollen endosomes and tubule formation in the endocytic recycling pathway is dramatically reduced, showing that both proteins are required for the transport of cargo such as the TfR from early endosomes to the endocytic recycling compartment.

## Introduction

Endocytosis is essential for the uptake of vesicles containing receptor-bound nutrients and signalling receptors from the plasma membrane. After internalisation these vesicles are transported from the plasma membrane into the cell and fuse with the early endosome, where cargo such as signalling receptors are sorted into multivesicular endosomes for lysosomal degradation. Membrane pumps, channels and nutrient receptors, such as the transferrin receptor, are sorted into a recycling pathway back to the plasma membrane, either via a rapid loop from an early endosome or by a longer indirect route via the perinuclear endocytic recycling compartment (ERC) (Maxfield and McGraw, 2004). Although the exact molecular mechanisms involved in the delivery of receptors to the recycling compartment and the transport back to the cell surface remain to be elucidated, the small GTPase Rab11 and the eps15 homology domain (EHD) family of proteins have been implicated in controlling this membrane trafficking pathway (Ullrich et al., 1996) (Sonnichsen et al., 2000) (Naslavsky and Caplan, 2005) (Naslavsky et al., 2006). The actin-based motor protein myosin Vb has also been reported to associate with Rab11 and to regulate transport of receptors out of the perinuclear ERC back to the cell surface (Hales et al., 2002) (Lapierre et al., 2001) (Roland et al., 2007).

Address all correspondence to Folma Buss, Cambridge Institute for Medical Research, University of Cambridge, Wellcome Trust/MRC Building, Hills Road, Cambridge CB2 2XY, UK. Tel +1223 (office) 763225 (lab) 336782, Fax +1223 762640, Email: fb1@mole.bio.cam.ac.uk.


Europe PMC Funders Author Manuscripts

We show here that another class of myosins is required for the delivery of cargo from the early endosome into the endocytic recycling compartment. Class VI myosins play crucial role(s) in membrane trafficking pathways, because they are the only class that so far has been shown to move “backwards” towards the minus end of actin filaments, in the opposite direction to all other myosins so far characterised (Wells et al., 1999). Myosin VI is associated with secretory and endocytic membrane compartments (Buss et al., 2001; Buss et al., 1998; Warner et al., 2003) (Aschenbrenner et al., 2003) and several binding partners, responsible for myosin VI’s differential intracellular targeting/recruitment, have now been identified. In the early endocytic pathway recruitment of myosin VI to clathrin coated structures at the plasma membrane requires Dab2 (Disabled-2) (Morris et al., 2002) (Spudich et al., 2007) and to uncoated endocytic vesicles requires GIPC (GAIP interacting protein C-terminus) (Bunn et al., 1999) (Naccache et al., 2006). Myosin VI function in exocytic membrane trafficking pathways needs the Rab8 effector protein optineurin, which links myosin VI to the Golgi complex (Sahlender et al., 2005). In polarized epithelial cells myosin VI is required for the transport of newly synthesized membrane proteins containing a tyrosine-sorting motif to the basolateral domain. These membrane proteins are sorted on route to the basolateral plasma membrane in the endocytic recycling endosome (Ang et al., 2004), where myosin VI and optineurin together with Rab8 and the transferrin receptor have been localised (Au et al., 2007).

In this study we have identified LMTK2 (lemur tyrosine kinase 2) (also known as cprk, KPI-2, BREK, Lmr2, AATYK2 and KIAA1079) as a myosin VI binding partner and have investigated the role(s) of the LMTK2-myosin VI complex in endocytic and exocytic membrane trafficking pathways. LMTK2 is a member of the lemur kinase group and is a Ser/Thr specific protein kinase with two predicted transmembrane domains at its N-terminus, followed by a kinase domain and a very long C-terminal tail domain (Wang and Brautigan, 2002) (Kesavapany et al., 2003) (Kawa et al., 2004). LMTK2 was previously identified as a binding partner of p35 - activator subunit for cyclin-dependent kinase 5 (Kesavapany et al., 2003) and as a binding partner for protein phosphatase 1C and its small inhibitor protein 2 (Wang and Brautigan, 2002). Several potential LMTK2 substrates have been identified: protein phosphatase 1C (Wang and Brautigan, 2002), phosphorylase b and the cystic fibrosis transmembrane conductance regulator (CFTR) (Wang and Brautigan, 2006). Mutations in the CFTR gene are linked to the genetic disorder cystic fibrosis (Rommens et al., 1989) (Riordan et al., 1989). Interestingly, myosin VI is required for endocytosis of CFTR from the apical domain of polarized epithelial cells (Swiatecka-Urban et al., 2004) (Ameen and Apodaca, 2007) and here we show that myosin VI binds directly to LMTK2, which can potentially phosphorylate CFTR.

LMTK2 is the first transmembrane protein and kinase that binds directly to myosin VI. Our functional studies demonstrate that both proteins, myosin VI and LMTK2, are required for delivery of cargo such as the transferrin receptor from the early endosome to the endocytic recycling compartment.

## Results

### LMTK2 is a novel myosin VI binding partner

Myosin VI was identified in a yeast two-hybrid screen as a LMTK2 binding partner using the LMTK2 cytoplasmic domain (residue 67 to the end of the C-terminus) as a bait to probe a human brain cDNA library. About half of positive clones identified in this screen encoded the C-terminal tail of myosin VI. To confirm and further investigate the interaction between myosin VI and LMTK2 we used a mammalian two-hybrid assay. Using this system we have previously mapped the binding sites for three other myosin VI binding partners at two independent sites in the C-terminal domain of the myosin VI tail: Dab2 binding requires a

WWY motif, whereas the GIPC and optineurin binding site contains a RRL motif (Sahlender et al., 2005) (Spudich et al., 2007). To determine the region on myosin VI involved in LMTK2 binding, we tested a range of point mutants and established that binding of LMTK2 to myosin VI tail requires the WWY motif, the same site used by Dab2 (Fig. 1B, C). Mutations in the RRL motif in the myosin VI tail (the binding site for optineurin) did not affect its binding to LMTK2 (data not shown). By testing multiple LMTK2 deletion mutants we identified a minimal fragment of about 200 amino acids (between aa 567 and 773) downstream of the kinase domain, which mediates interaction between the myosin VI tail and LMTK2 (Fig. 1A). Interestingly, myosin VI binds in a region that is different to the one identified for protein phosphatase 1 and its small inhibitor protein 2 (aa 1344-1450, Wang and Brautigan, 2002) but in the same region as p35, the activator subunit of cdk5 (aa 391-632, Kesavapani et al, 2003).

Myosin VI exists as four splice isoforms due to a large and small inserts in the tail region (Fig. 1B) and these isoforms have been shown to have distinct role in membrane trafficking pathways (Buss et al., 2001) (Au et al., 2007). So we tested the binding of LMTK2 to these different splice isoforms of myosin VI. LMTK2 binds to the myosin VI tail regardless of whether it contains the large (31 aa) insert or not, however it shows slightly stronger binding when this insert is present (Fig. 1D). This result suggests that LMTK2, which is a ubiquitously expressed kinase, is able to interact with the different myosin VI isoforms that are expressed in a variety of different tissues and cells (Buss et al., 2001).

To confirm that myosin VI directly binds to LMTK2 we used a GST-pull down assay. An *in vitro* translated [$^{35}$S]methionine-labelled LMTK2 fragment (aa 451-1095) was incubated with either GST alone, the wild type GST-myosin VI tail or a mutant GST-myosin VI tail (WWY->WLY) (Fig. 2A). Whereas LMTK2 strongly binds to the wild type myosin VI tail, no binding to GST alone and only very weak binding to the mutant myosin VI tail (WWY->WLY) was observed. These results support the observation that binding of LMTK2 and Dab2 to the myosin VI tail involves the WWY motif and that myosin VI binds directly to LMTK2.

Finally, we confirmed the interaction between myosin VI and LMTK2 *in vivo* by coimmunoprecipitation using affinity purified polyclonal antibodies to either myosin VI tail or the cytoplasmic tail of LMTK2. As shown in Fig. 2B, endogenous myosin VI coimmunoprecipitates with a small amount of LMTK2, however overexpression of GFP-tagged myosin VI leads to a substantial increase in the amount of LMTK2 found in a complex with myosin VI. In the reciprocal experiment antibodies to LMTK2 can also immunoprecipitate myosin VI from HeLa cells that express GFP-myosin VI (Fig. 2C). These results demonstrate that myosin VI and LMTK2 exist together in a protein complex within the cell.

## Intracellular localisation of LMTK2 and myosin VI

To investigate whether myosin VI and LMTK2 localise to the same intracellular compartment, myosin VI tagged with GFP and untagged LMTK2 were coexpressed in HeLa cells and these cells were labeled with a polyclonal antibody to LMTK2 and a monoclonal antibody to GFP. LMTK2 was present at the plasma membrane, in a vesicular staining pattern throughout the cell, but concentrated in cell extensions and in the perinuclear area (Fig. 3, 4). GFP-tagged myosin VI was found to colocalise with LMTK2 in small punctate structures throughout the cell (Fig. 3A). Myosin VI and LMTK2 only partially colocalise probably because LMTK2 is not the only myosin VI binding partner present in the cell and both proteins may have overlapping but distinct intracellular functions. To see whether endogenous myosin VI also colocalises with LMTK2, LMTK2 transfected cells were stained with antibodies to myosin VI. Endogenous myosin VI colocalised with LMTK2 on

small vesicles (Fig. 3B). In the reverse experiment however we were unable to detect endogenous LMTK2, which probably reflects the low expression level of this kinase.

Are the vesicles containing myosin VI and LMTK2 involved in the endocytic or the exocytic membrane trafficking routes? Previously, we demonstrated that myosin VI is present at/around the Golgi complex and plays a role in constitutive secretion (Warner et al., 2003) (Sahlender et al., 2005). LMTK2 was also reported to be concentrated in the perinuclear region of the cell at the Golgi complex (Kesavapany et al., 2003). However, we found very little overlap between LMTK2 and GM130, a marker protein of the Golgi matrix (supplementary materials Fig. S1A). In siRNA knockdown experiments, cells depleted of myosin VI showed (as expected) a dramatic reduction in constitutive secretion of the reporter molecule, secreted alkaline phosphatase (SEAP), however, cells depleted of LMTK2 displayed no reduction in the level of SEAP secretion when compared to control cells (supplementary material Fig. S1B). Similarly, the transport of tsVSV-G from the Golgi complex to the cell surface was not affected in LMTK2 knockdown cells (supplementary material Fig. S1C). These results indicate that LMTK2 does not play a major role in the secretory pathway.

To test the involvement of LMTK2 in the endocytic pathway, GFP-tagged LMTK2 was transfected into HeLa cells, which were pulsed with fluorescently labeled transferrin for 20 min to allow uptake of transferrin into peripheral endocytic structures and the endocytic recycling compartment. Figure 4(a-c) demonstrates that LMTK2 is present on transferrin-positive endocytic structures. Double labelling experiments show that LMTK2 is present on a subset of early endosomes as revealed by colocalisation with Rab5 and EEA1 (Fig. 4, d-j) and also associated with the Rab11-positive endocytic recycling compartment (Fig. 4, k-m).

In agreement with previous studies in unpolarised cells we observed myosin VI concentrating on uncoated vesicles, where it colocalises with GIPC and the early endosomal marker Rab5, but hardly any myosin VI colocalises with EEA1 (supplementary material Fig. S2).

These results show that LMTK2 can be found along the early endocytic and recycling pathway, where it colocalises with Rab5, EEA1 and Rab11, whereas myosin VI displays a more restricted localization, being concentrated in the early endocytic pathway on Rab5 positive early endosomes.

## Loss of myosin VI and LMTK2 leads to enlarged endosomes

To address the function of LMTK2 and myosin VI in the endocytic and recycling pathway, we reduced the cellular expression levels of these proteins using small interfering RNA (siRNA). HeLa cells were transfected twice with either control oligo or siRNAs specific for LMTK2 or myosin VI. Immunoblot analysis showed that 48 h after the second transfection the expression levels of LMTK2 and myosin VI were down to less than 5% as compared to control cells (Fig. 5A). To study the effects of LMTK2 or myosin VI depletion, we processed the knockdown (KD) and control cells for immunofluorescence microscopy to visualise the steady-state localisation of endocytic organelles. The fixed cells were labeled with antibodies against the early endosomal marker EEA1 and against vps26, a component of the mammalian retromer complex, which is present on early and late endosomes and is important for retrieval of transmembrane proteins from endosomes back to the Golgi complex. In control cells early and late endosomes are represented by small vesicles dispersed through out most of the cell with a slight concentration in the perinuclear region (Fig. 5B). However, in cells transfected with siRNAs specific for myosin VI or LMTK2, EEA1 and vps26 are now present in large swollen, ring-like endosomes, which often aggregate in the perinuclear region. This phenotype was most dramatic in myosin VI KD

cells, where hardly any small endocytic structures were found in the cell periphery. LMTK2 KD cells displayed identical changes in endosome morphology, however, the redistribution into a tight spot in the perinuclear area was not always as dramatic as in myosin VI depleted cells.

To follow the uptake of transferrin into the control and KD cells we pulsed the cells for 20 min with fluorescently labeled transferrin. In control cells transferrin was found in peripheral endocytic structures and was also present in the perinuclear endocytic recycling compartment, whereas in myosin VI and LMTK2 KD cells the transferrin was trapped in swollen endocytic vesicles (Fig. 5C), which were positive for EEA1 (supplementary material Fig. S3) and vps26 (data not shown).

## Myosin VI and LMTK2 are required for transport of transferrin from early endosomes to the endocytic recycling compartment (ERC)

After endocytosis and delivery to an early endocytic compartment the transferrin receptor is either recycled directly from the early endosome back to the plasma membrane or it is delivered to a morphologically distinct endocytic recycling compartment (Fig. 9) and for review see (Maxfield and McGraw, 2004). This compartment has been described as a perinuclear collection of tubular/vesicular membranes containing Rab11 (Hopkins and Trowbridge, 1983) (Yamashiro et al., 1984). Since the loss of myosin VI and LMTK2 expression causes the accumulation of the transferrin receptor in swollen organelles containing the early endosomal marker EEA1, we tested whether this receptor is still delivered to the Rab11 positive ERC in myosin VI and LMTK2 knockdown cells. A stable cell line expressing GFP-tagged Rab11 was either mock treated or transfected with myosin VI or LMTK2 siRNA and immunostained with antibodies to GFP and the tranferrin receptor. As shown in Fig. 6 in mock treated cells the endogenous transferrin receptor is present in the cell periphery, but also in the perinuclear region and on tubules emanating from the centre towards the periphery of the cell. These control cells show a high degree of colocalisation between the transferrin receptor and Rab11, a marker of the ERC. In myosin VI and LMTK2 KD cells the transferrin receptor is trapped in swollen endosomes, consistant with the results from the fluorescently labelled tranferrin uptake experiment, but now shows very little colocalisation with Rab11 and the ERC (Fig. 6A), indicating that the transferrin receptor does not reach the ERC.

In addition, we investigated the effect of myosin VI and LMTK2 depletion on the late endocytic pathway. We observed no accumulation of the lysosomal marker lamp1 in transferrin-positive endosomes as well as no defects in ligand induced EGFR degradation in either of the knockdowns (supplementary material Fig. S4).

These results suggest that myosin VI and LMTK2 play a role in the transport of cargo from the early endosome to the perinuclear recycling compartment.

## Loss of myosin VI and LMTK2 causes a delay in recycling of transferrin receptor to the plasma membrane

We used FACS analysis to measure intracellular trafficking of TfR in control and siRNA treated cells (see details in Methods and corresponding figure legends).

To determine whether the loss of myosin VI or LMTK2 expression not only inhibits delivery of the transferrin receptor to the ERC but also affects its recycling back to the plasma membrane, we pulsed mock and siRNA treated cells with fluorescently labelled transferrin at 37°C, followed by a chase for different times in the presence of excess unlabelled transferrin to allow recycling. Comparing the amount of transferrin left in cells

revealed small but consistent defects in TfR recycling to the cell surface in both myosin VI and LMTK2 depleted cells (Fig. 6B).

To address a possible role of myosin VI and LMTK2 in fast recycling pathway, we used two approaches. Firstly, we loaded cells with Tf-Alexa647 at 16°C and allowed them to recycle at 37°C. Temperatures below 20°C have been shown to accumulate transferrin receptor in sorting endosomes and prevent its transport to perinuclear recycling compartment (Ren et al., 1998). Secondly, we pulsed cells with transferrin at 37°C for 5 minutes before recycling at 37°C. During the short pulse, transferrin only reaches the early endocytic vecicles and not the perinuclear recycling compartment. Using either method we observed a reduction in fast recycling in myosin VI depleted cells, but no reduction and even a slight increase in fast recycling in cells depleted of LMTK2 (supplementary material Fig S5, A-B).

We also observed a reduction in the total amount of transferrin internalised in myosin VI and LMTK2 knockdown cells (supplementary material Fig S5, C-D), which could reflect accumulation and trapping of TfR in the swollen endocytic compartment. However, the total amount of TfR measured by FACS (supplementary material Fig S5, E) and by Western blot (data not shown) appeared to be reduced in both myosin VI and LMTK2 depleted cells, which could explain the observed reduction in total transferrin internalised.

## Tubule formation in the endocytic recycling pathway is inhibited in the absence of myosin VI or LMTK2

In the GFP-Rab11 stable cell line the transferrin receptor is present in an array of long tubules, which are probably transport intermediates, containing Rab11 that emerge from the perinuclear region and extent into the periphery of the cell. In myosin VI and LMTK2 KD cells we noticed a dramatic reduction of Rab11 positive tubules emanating from the perinuclear area and at the same time there was a collapse of Rab11 into a tighter perinuclear spot. Otherwise, the overall distribution of Rab11 in the cell periphery and in cell extensions at the plasma membrane was unchanged (Fig. 7A). To quantify this observation the number of cells containing Rab11 positive tubules was scored in mock treated cells and compared to the number in myosin VI or LMTK2 KD cells. In control cells about half the cells (46%) had obvious Rab11 tubules, whereas only 13% of the myosin VI KD and 26% of the LMTK2 KD cells contained any Rab11 positive tubules (Fig. 7B). These results suggest that tubule formation for cargo recycling back to the plasma membrane is dramatically inhibited in myosin VI and LMTK2 KD cells.

To verify this observation we investigated the formation of EHD1 or EHD3 containing tubules in cells depleted of myosin VI or LMTK2. EHD1 and EHD3 belong to the Eps15 homology domain (EHD) family of proteins that are part of the Rab11 mediated endocytic recycling pathway (Naslavsky and Caplan, 2005). Whereas EHD1 appears to regulate transport of a number of different receptors from the endocytic recycling compartment to the plasma membrane (Caplan et al., 2002; Lin et al., 2001; Naslavsky et al., 2004; Picciano et al., 2003), EHD3 plays a role in the delivery of cargo from the early endosome to the ERC (Naslavsky et al., 2006). Both proteins are found on vesicles and long membrane tubules associated with the ERC and the Rab11 recycling pathway. To determine whether loss of myosin VI or LMTK2 affects formation of EHD1- or EHD3-positive tubules, we used a stable HeLa cell line expressing either GFP-EHD1 or GFP-EHD3. In GFP-EHD1 expressing cells treated with myosin VI siRNA very few cells containing long EHD1-tubules were observed, instead the EHD1 was present in large vesicular structures in the cell periphery. LMTK2 KD cells also displayed a very dramatic reduction in the number of EHD1-positive tubules (Fig. 8A). Reduced expression levels of myosin VI and LMTK2 had a very similar effect on EHD3-positive tubule formation (Fig. 8B). To quantify the reduction in the number of EHD3 tubules, the number of cells containing either no tubules, a few (<15) tubules or

multiple (>15) tubules were counted (Fig. 8C). The majority of the mock treated cells contained multiple tubules, whereas in the myosin VI KD cells more than 50% of them contained no EHD3-positive tubules at all, and in LMTK2 KD cells a dramatic reduction in the number of cells containing multiple tubules was also observed. We looked at the cells, which did have tubules in the three experimental conditions (mock and both KDs) and counted the number of tubules per cell and measured the length of individual tubules. As shown in Fig. 8D, in both myosin VI and LMTK2 knockdown cells, there was a shift in the distribution towards having fewer tubules (dramatic in myosin VI KD and considerable in LMTK2 KD). Only minor difference in the lengths of the tubules in KD cells compared to control was observed (Fig. 8E).

In conclusion our results indicate that LMTK2 is a novel binding partner of myosin VI. Both proteins are required for delivery of the TfR to the endocytic recycling compartment and are part of the membrane trafficking machinery in the endocytic recycling pathway (Fig. 9).

## Discussion

We identified LMTK2 as a novel myosin VI interacting protein, the first membrane protein that has been shown to directly bind to myosin VI. LMTK2 is a member of a family of serine/threonine kinases with a N-terminal transmembrane domain and a long cytoplasmic tail containing the catalytic domain. The interaction between myosin VI and LMTK2 was first discovered in a yeast two-hybrid screen and confirmed in a variety of different protein-protein interaction assays *in vitro* and *in vivo*. Our localisation studies show that LMTK2 is present on transferrin, Rab5, EEA1 and Rab11 positive structures along the endocytic and recycling pathway. Myosin VI is found in the early endocytic pathway close to the plasma membrane on Rab5 positive endosomes, but in contrast to LMTK2 very little myosin VI is present on EEA1 or Rab11 positive vesicles (supplementary material Fig. S2 and data not shown). The broader distribution of LMTK2 along the endocytic pathway and restricted localisation of myosin VI in the early pathway might explain the limited colocalisation of these two proteins. In addition, both proteins were shown to have separate and probably independent functions in the cell (Sahlender et al., 2005) (Kawa et al., 2004).

LMTK2 binds to the WWY motif in the C-terminal tail of myosin VI and therefore shares a binding site with Dab2. This binding site is distinct from the RRL motif, where optineurin and GIPC bind in the C-terminal tail of myosin VI. Dab2 links myosin VI to the very first steps in the endocytic pathway involving clathrin mediated vesicle formation at the plasma membrane, whereas GIPC has been implicated in myosin VI driven transport of uncoated early endocytic vesicles through the cortical actin network in epithelial cells (Aschenbrenner et al., 2003). LMTK2 is thus the third myosin VI binding partner implicated in endocytic membrane trafficking.

Aschenbrenner et al. (2003) observed that ablating myosin VI activity by overexpressing of the dominant negative myosin VI tail leads to accumulation of transferrin positive vesicles in the cortical actin network. In our experiments we also observed a slight delay in trafficking of transferrin containing vesicles through the peripheral actin network in myosin VI KD cells (data not shown), however, the transferrin receptor still reached and accumulated in swollen early endosomes. The major defect we observed in myosin VI KD cells was therefore not the retention of uncoated endocytic vesicles in the cell periphery, but a block in transport of transferrin receptor from the early endosomes to the endocytic recycling compartment.

In the majority of the experiments, where myosin VI expression was suppressed, there was a slightly more dramatic phenotype than when LMTK2 expression was lost, although similar

levels of KD were achieved for both proteins (Fig. 5A). In myosin VI KD cells the loss of Rab11-, EHD1- and EHD3-positive tubules was more severe and transferrin recycling was inhibited to a greater extent. Since LMTK2 is a Ser/Thr kinase and only small amounts of it maybe required to phosphorylate its target proteins and to fulfil its intracellular roles, it may be necessary to completely deplete it in order to see a dramatic effect. However, overall we observed a very similar phenotype in myosin VI and LMTK2 KD cells, which strongly suggest that both proteins act in a functional complex in the endocytic pathway. Since LMTK2 is a transmembrane protein it might be involved in recruiting myosin VI to the surface of the endosome or as a protein kinase it could be involved in regulating myosin VI function by phosphorylation or myosin VI could transport the kinase to the appropriate compartment so that it could phosphorylate its target proteins.

Several possible phosphorylation sites have been identified in myosin VI. Phosphorylation of two threonines in the C-terminal tail region ($T_{1089}INT_{1092}$) has been shown to regulate optineurin binding to the myosin VI tail (Sahlender et al., 2005). In addition myosin VI contains a conserved threonine residue ($T_{405}$) in the actin binding interface in the motor domain and its phosphorylation plays a crucial role in regulating the activity of myosin I (Bement and Mooseker, 1995). Although phosphorylation at this site does not change the *in vitro* kinetic properties of the motor (Morris et al., 2003), it might modulate myosin VI-actin interaction, when phosphorylated *in vivo* (Buss et al., 1998) (Naccache and Hasson, 2006). To investigate whether LMTK2 is able to phosphorylate myosin VI *in vitro*, we performed phosphorylation experiments using purified baculovirus expressed myosin VI and LMTK2 immunoprecipitated from HeLa cells. So far under the condition tested (see supplementary material), we have not been able to demonstrate that myosin VI is phosphorylated by LMTK2. However, the full-length LMTK2 tested after being released from membranes using detergent and immunoprecipitated from HeLa cells may not be fully active. In addition LMTK2 activity has been shown to be regulated by nerve growth factor as well as by direct phosphorylation by cdk5 (Kawa et al., 2004) (Kesavapany et al., 2003). The level of phosphorylation of GFP-myosin VI immunoprecipitated from cells transfected either with wildtype LMTK2 or a kinase-dead LMTK2 was also tested, but so far we have been unable to detect significant differences in myosin VI phosphorylation (data not shown).

The major phenotype observed in myosin VI and LMTK2 KD cells is a block in TfR trafficking from early endosomes to the ERC. This defect is very similar to the phenotype observed in EHD3 knockdown cells, where delivery of internalised transferrin to the ERC is blocked and there is an accumulation of cargo in the EEA1 positive early endosome. In these cells, like in the myosin VI and LMTK2 KD cells, only a slight delay in transferrin recycling was measured (Naslavsky et al., 2006). Other studies (Hirst et al., 2005) have suggested that blocking TfR delivery to the ERC might redirect it into the direct fast recycling pathway from the early endosome back to the plasma membrane (see model in Fig. 9). We observed only very slight upregulation of fast recycling in LMTK2 depleted cells, which may partially compensate for the defect in trafficking through the ERC. However, in myosin VI knockdown cells both fast and slow recycling are slightly reduced, a phenotype similar to that observed in cells overexpressing dominant negative Rab11S25N (Ullrich et al., 1996) (Ren et al., 1998). These results indicate that myosin VI affects delivery into both fast and slow recycling pathways.

Our results suggest a role for myosin VI and LMTK2 at the early endosome for delivery of cargo to the ERC. Further support for this proposal is the observation that siRNA KD of myosin VI and LMTK2 have a dramatic effect on EHD3 tubule formation. However, whether loss of EHD3 tubule formation is the primary cause for reduced transport to the ERC needs to be established. The loss of EHD1 and Rab11 tubules emerging from the ERC in the myosin VI and LMTK KD cells suggests that either these proteins have a role at the

recycling endosome or it could be a secondary effect due to the reduced transport of cargo into the ERC. However, we have recently shown that myosin VI functions in the recycling compartment in MDCK cells (Au *et al.*, 2007). In these polarised epithelial cells myosin VI is present in recycling endosomes, where it is required for sorting of AP-1B dependent cargo to the basolateral domain. Therefore, myosin VI might play a role in the recycling compartment not only in polarised and but also in nonpolarised cells.

LMTK2 knockout mice are apparently normal at birth, but adult -/- males are infertile (Kawa et al., 2006). Closer investigation revealed that LMTK2-/- mice have defects in spermatogenesis, particularly in the formation of the acrosome. Although the exact molecular mechanisms involved in acrosome formation are not known, it has been shown that it requires membrane trafficking for acrosomal proteins to be sorted and delivered into the growing acrosome (Moreno et al., 2000) (Ramalho-Santos et al., 2002). It would be interesting to look more closely at other specialised cell types in this knockout mouse and compare their phenotypes to those in the myosin VI (Snell's waltzer) knockout mouse.

In this paper we have established that the myosin VI-LMTK2 complex is a new player in the endocytic recycling pathway, since both proteins play a crucial role in trafficking of cargo from the early endosome to the ERC and in tubule formation from the ERC. Whether myosin VI and LMTK2 are involved in the formation of transport vesicles or tubules or whether they play a role in recruitment of proteins/cargo into transport carriers or whether myosin VI transports LMTK2 to its target proteins are some of the intriguing questions that remain to be answered.

## Materials and Methods

### Expression constructs and antibodies

The LMTK2/pCIneo (Cprk/pCIneo) construct expressing human LMTK2 amino acids 1-1443 was previously described (Kesavapany et al., 2003) and the LMTK2 aa 1-1503 construct (pCMV-KPI-2) (Wang and Brautigan, 2002) provided by D. Brautigan (University of Virginia). To create the LMTK2-GFP fusion the LMTK2 (aa 1-1503) was cloned into *Xho*I and *BamH*I sites of pEGFPN1 (Clontech). Human myosin VI constructs with (MyoVI-LI) and without (MyoVI-NI) the insert in the tail domain were previously described (Sahlender et al., 2005; Spudich et al., 2007).

To generate the constructs for stable expression, human Rab11 cDNA (purchased from University of Missouri-Rolla cDNA Resource Center) and mouse EHD1 and EHD3 (EST cDNAs obtained from the IMAGE Consortium) were cloned into pEGFPC1 vector and then the GFP-fusion cassettes were subcloned into pIRESneo2 (Clontech).

The following antibodies were used: rabbit polyclonal to GFP (Molecular Probes), monoclonal to GFP (3E6, Qbiogene), monoclonals to EEA1, Rab 5 and GM130 (BD Transduction Laboratories), monoclonal to transferrin receptor (Zymed), monoclonal to alpha-tubulin (Sigma), polyclonal to EGFR (Santa Cruz), monoclonal to LAMP1 (Developmental Studies Hybridoma Bank, University of Iowa), polyclonal to GIPC (Proteus Biosciences), polyclonals to myosin VI tail (Buss et al., 1998) and Vps26 (Seaman, 2004). Rabbit polyclonal antibodies to LMTK2 were generated by immunization with a GST-LMTK2 fusion protein (aa 996-1443) and affinity purified using antigen-CNBr-Sepharose chromatography (GE Biosciences).

### Two-hybrid assays

The yeast two-hybrid screen was performed using the cytoplasmic domain of LMTK2 (aa 67-1443) as the bait cloned into pY1. A pre-transformed human brain MatchMaker library

(Clontech) was screened with LMTK2 as the bait according to the manufacturers instructions. The interaction between myosin VI and LMTK2 identified in the yeast two-hybrid screen was confirmed in the mammalian two-hybrid assay using the human myosin VI tail (containing the large insert, aa 840-1284) as the bait and the LMTK2 cytoplasmic tail as the prey. The human myosin VI tail was used as a template to generate point mutations WWY->WLY (aa 1191-1193) and RRL->AAA (aa 1115-1117) using a QuickChange protocol (Stratagene). The mutant tail fragments were cloned into the "bait" vector pM (Clontech). A series of LMTK2 deletion mutants (Fig. 1A) were cloned into the "prey" vector pVP16 (Clontech). CHO cells 6-well plates were transfected with 1$\mu$g of both bait and prey vectors together with 0.8 $\mu$g each of the reporter plasmids, pG5luc (Clontech), coding for inducible firefly luciferase, and pRL-CMV (Promega), coding for the constitutively active Renilla luciferase. After 72 hours the relative luciferase activity was assayed using Dual-Luciferase Reporter Assay System (Promega).

### Cell culture and transfection

CHO, HeLa and RPE cells were cultured in F-12 HAM, RPMI 1640 and DMEM/F-12 medium respectively, containing 10% fetal calf serum, 2mM L-glutamine, 100U/ml penicillin and 100$\mu$g/ml streptomycin. Cells were transfected using FuGENE (Roche Diagnostics) according to the manufacturer's instruction.

To generate GFP-Rab11, GFP-EHD1 and GFP-EHD3 stably expressing cell lines, HeLa cells were transfected with corresponding constructs in pIRESneo2 and selected with complete medium containing 500$\mu$g/ml G418 (Gibco).

### Immunoprecipitation

Hela cells growing in 10 cm plates were transfected with the GFP-MyoVI-NI construct and 36-48 hours later lysed in extraction buffer containing 50 mM TRIS pH 7.5, 100 mM NaCl, 20 mM NaF, 20 mM $Na_4P_2O_7$, 5 mM $MgCl_2$, 5 mM ATP, 1 mM activated Na-*o*-vanadate, 1% Igepal CA-630 and protease inhibitor cocktail (Roche). The lysate was cleared by centrifugation (13000×g, 15 min) and immunoprecipitation was performed as described previously (Buss at el., 1998). For immunoprecipitation rabbit polyclonal antibody to the tail domain of myosin VI or to LMTK2 residues 996-1443 were used. Non-immune rabbit serum was used as a negative control in all experiments. Immunoprecipitated complexes were washed 5 times in extraction buffer and analysed by SDS-PAGE followed by immunoblotting. Blots were developed using ECL detection reagent (Amersham).

### GST pull-down assay

The GST-chicken myosin VI tail (aa 840-1277) was expressed and purified as described (Buss et al., 1998). LMTK2 fragment (aa 451-1095) was cloned into pcDNA3 (Invitrogen) and transcribed and translated *in vitro* in the presence of [$^{35}$S]-methionine using the TNT-coupled Reticulocyte Lysate System (Promega). The [$^{35}$S]-labelled LMTK2 fragment was incubated with 5$\mu$g of GST or GST-myosin VI tail on glutathione beads in 10 mM HEPES pH 7.4, 150 mM NaCl, 1% Triton X-100 at 4°C for 2 hours. After extensive washing the protein complexes bound to glutathione beads were separated by SDS PAGE and analysed by autoradiography.

### siRNA knockdowns

OligofectAMINE (Invitrogen) was used for siRNA transfection. For efficient knockdown of myosin VI and LMTK2 Hela cells were transfected twice with siRNA on day 1 and 3. On day 5 cells were processed for immunofluorescence and the efficiency of protein depletion was assessed by Western blotting. Mock treated cells and cells transfected with scrambled

siRNA oligo were used as controls. All siRNA oligos were obtained from Dharmacon. Human myosin VI was targeted with ON-TARGETplus Smart pool siRNA, all four oligos tested separately gave the same level of myosin VI depletion and the same phenotype. LMTK2 was targeted with either oligo 2068: UCAGGAGCGUUGAACUUGAUU, or the following ON-TARGETplus oligos: 1158: GCAGGUACAAGGAGGAUUAUU, 1262: GCAGAUCAGACUAAGUAUAUU, 1972: GUAGUAACUUGGAGCUUGAUU. All four oligos gave the same level of protein depletion and the same phenotype. Most LMTK2 knockdown experiments presented in the manuscript were performed using a mixture of four of the above listed oligos.

### Immunofluorescence

HeLa cells growing on coverslips were transfected with corresponding plasmids and 48 hours later were fixed with 4% PFA, permeabilised with 0.1% Triton, blocked with 1% BSA in PBS and processed for indirect immunofluorescence using primary antibodies (specified in the Fig. legends) and secondary antibodies coupled with Alexa488 or Alexa555 (Molecular Probes). In siRNA knockdown experiments, the cells were plated on coverslips on day 4 and on day 5 fixed and processed for immunofluorescence as described above. The cells were visualised with a Zeiss Axioplan epifluorescence microscope or Zeiss LSM-510 confocal (Carl Zeiss MicroImaging Inc.). For transferrin uptake experiments, cells were starved in RPMI containing 0.2% BSA for 2 hours, loaded with 5 $\mu$g/ml Tf-Alexa555 (Molecular Probes) in RPMI-0.2% BSA for 20 minutes at 37°C, washed in PBS and fixed.

To quantify Rab11 or EHD3-positive tubules, the images of cells containing tubules were taken on Zeiss Axioplan epifluorescence microscope using 100x objective. The number and length of individual tubules were measured manually. Branches were considered as individual tubules.

### FACS-based endocytosis assays

Transferrin uptake and recycling assays were performed as previously described (Peden et al., 2004). Briefly, for recycling assays, the cells were incubated with Tf-Alexa647 (Molecular Probes) for 30 min at 4°C followed by internalisation at 37°C or 16°C in the continuous presence of Tf-Alexa647. Cells were then washed and incubated at 37°C in media supplemented with 100$\mu$g/ml unlabelled transferrin for various times before fixation in 3.7% PFA. Cell-associated Tf-Alexa647 was determined by FACS analysis using BD FACSCalibur flow cytometer (BD Biosciences).

## Supplementary Material

Refer to Web version on PubMed Central for supplementary material.

## Acknowledgments

We thank Dr Valerie Cullen for performing the yeast-two hybrid screen that identified myosin VI as a LMTK2 binding partner, S. Arden for testing the interaction in GST-pulldown assays, Dr C. Puri for creating Rab11-GFP cell line, Dr S. Gokool for providing GFP-EHD1 and GFP-EHD3 cell lines, Dr A. Peden for help with transferrin uptake assays. We also would like to thank Prof J.P. Luzio for help and advice. We are grateful to Dr D. Brautigan (University of Virginia) for the full-length LMTK2 construct. This work was funded by a Wellcome Trust Senior Fellowship (F.B.), a MRC Senior Fellowship (M.N.J.S.) and supported by the Medical Research Council (J.K-J. and C.C.M.), BBSRC, MNDA and European Union NeuroNE (C.C.M.). CIMR is in receipt of a strategic award from the Wellcome Trust.

## References


Ameen N, Apodaca G. Defective CFTR apical endocytosis and enterocyte brush border in myosin VI-deficient mice. Traffic. 2007; 8:998–1006. [PubMed: 17555536]

Ang AL, Taguchi T, Francis S, Folsch H, Murrells LJ, Pypaert M, Warren G, Mellman I. Recycling endosomes can serve as intermediates during transport from the Golgi to the plasma membrane of MDCK cells. J Cell Biol. 2004; 167:531–43. [PubMed: 15534004]

Aschenbrenner L, Lee T, Hasson T. Myo6 facilitates the translocation of endocytic vesicles from cell peripheries. Mol Biol Cell. 2003; 14:2728–43. [PubMed: 12857860]

Au JS, Puri C, Ihrke G, Kendrick-Jones J, Buss F. Myosin VI is required for sorting of AP-1B-dependent cargo to the basolateral domain in polarized MDCK cells. J Cell Biol. 2007; 177:103–14. [PubMed: 17403927]

Bement WM, Mooseker MS. TEDS rule: a molecular rationale for differential regulation of myosins by phosphorylation of the heavy chain head. Cell Motil Cytoskeleton. 1995; 31:87–92. [PubMed: 7553910]

Bunn RC, Jensen MA, Reed BC. Protein interactions with the glucose transporter binding protein GLUT1CBP that provide a link between GLUT1 and the cytoskeleton. Mol Biol Cell. 1999; 10:819–32. [PubMed: 10198040]

Buss F, Arden SD, Lindsay M, Luzio JP, Kendrick-Jones J. Myosin VI isoform localized to clathrin-coated vesicles with a role in clathrin-mediated endocytosis. Embo J. 2001; 20:3676–84. [PubMed: 11447109]

Buss F, Kendrick-Jones J, Lionne C, Knight AE, Cote GP, Paul Luzio J. The localization of myosin VI at the golgi complex and leading edge of fibroblasts and its phosphorylation and recruitment into membrane ruffles of A431 cells after growth factor stimulation. J Cell Biol. 1998; 143:1535–45. [PubMed: 9852149]

Caplan S, Naslavsky N, Hartnell LM, Lodge R, Polishchuk RS, Donaldson JG, Bonifacino JS. A tubular EHD1-containing compartment involved in the recycling of major histocompatibility complex class I molecules to the plasma membrane. Embo J. 2002; 21:2557–67. [PubMed: 12032069]

Hales CM, Vaerman JP, Goldenring JR. Rab11 family interacting protein 2 associates with Myosin Vb and regulates plasma membrane recycling. J Biol Chem. 2002; 277:50415–21. [PubMed: 12393859]

Hirst J, Borner GH, Harbour M, Robinson MS. The aftiphilin/p200/gamma-synergin complex. Mol Biol Cell. 2005; 16:2554–65. [PubMed: 15758025]

Hopkins CR, Trowbridge IS. Internalization and processing of transferrin and the transferrin receptor in human carcinoma A431 cells. J Cell Biol. 1983; 97:508–21. [PubMed: 6309862]

Kawa S, Fujimoto J, Tezuka T, Nakazawa T, Yamamoto T. Involvement of BREK, a serine/threonine kinase enriched in brain, in NGF signalling. Genes Cells. 2004; 9:219–32. [PubMed: 15005709]

Kawa S, Ito C, Toyama Y, Maekawa M, Tezuka T, Nakamura T, Nakazawa T, Yokoyama K, Yoshida N, Toshimori K, et al. Azoospermia in mice with targeted disruption of the Brek/Lmtk2 (brain-enriched kinase/lemur tyrosine kinase 2) gene. Proc Natl Acad Sci U S A. 2006; 103:19344–9. [PubMed: 17158803]

Kesavapany S, Lau KF, Ackerley S, Banner SJ, Shemilt SJ, Cooper JD, Leigh PN, Shaw CE, McLoughlin DM, Miller CC. Identification of a novel, membrane-associated neuronal kinase, cyclin-dependent kinase 5/p35-regulated kinase. J Neurosci. 2003; 23:4975–83. [PubMed: 12832520]

Lapierre LA, Kumar R, Hales CM, Navarre J, Bhartur SG, Burnette JO, Provance DW Jr. Mercer JA, Bahler M, Goldenring JR. Myosin vb is associated with plasma membrane recycling systems. Mol Biol Cell. 2001; 12:1843–57. [PubMed: 11408590]

Lin SX, Grant B, Hirsh D, Maxfield FR. Rme-1 regulates the distribution and function of the endocytic recycling compartment in mammalian cells. Nat Cell Biol. 2001; 3:567–72. [PubMed: 11389441]

Maxfield FR, McGraw TE. Endocytic recycling. Nat Rev Mol Cell Biol. 2004; 5:121–32. [PubMed: 15040445]

Moreno RD, Ramalho-Santos J, Sutovsky P, Chan EK, Schatten G. Vesicular traffic and golgi apparatus dynamics during mammalian spermatogenesis: implications for acrosome architecture. Biol Reprod. 2000; 63:89–98. [PubMed: 10859246]

Morris CA, Wells AL, Yang Z, Chen LQ, Baldacchino CV, Sweeney HL. Calcium functionally uncouples the heads of myosin VI. J Biol Chem. 2003; 278:23324–30. [PubMed: 12682054]

Morris SM, Arden SD, Roberts RC, Kendrick-Jones J, Cooper JA, Luzio JP, Buss F. Myosin VI binds to and localises with Dab2, potentially linking receptor-mediated endocytosis and the actin cytoskeleton. Traffic. 2002; 3:331–41. [PubMed: 11967127]

Naccache SN, Hasson T. Myosin VI altered at threonine 406 stabilizes actin filaments in vivo. Cell Motil Cytoskeleton. 2006; 63:633–45. [PubMed: 16917816]

Naccache SN, Hasson T, Horowitz A. Binding of internalized receptors to the PDZ domain of GIPC/synectin recruits myosin VI to endocytic vesicles. Proc Natl Acad Sci U S A. 2006; 103:12735–40. [PubMed: 16908842]

Naslavsky N, Boehm M, Backlund PS Jr. Caplan S. Rabenosyn-5 and EHD1 interact and sequentially regulate protein recycling to the plasma membrane. Mol Biol Cell. 2004; 15:2410–22. [PubMed: 15020713]

Naslavsky N, Caplan S. C-terminal EH-domain-containing proteins: consensus for a role in endocytic trafficking, EH? J Cell Sci. 2005; 118:4093–101. [PubMed: 16155252]

Naslavsky N, Rahajeng J, Sharma M, Jovic M, Caplan S. Interactions between EHD proteins and Rab11-FIP2: a role for EHD3 in early endosomal transport. Mol Biol Cell. 2006; 17:163–77. [PubMed: 16251358]

Peden AA, Schonteich E, Chun J, Junutula JR, Scheller RH, Prekeris R. The RCP-Rab11 complex regulates endocytic protein sorting. Mol Biol Cell. 2004; 15:3530–41. [PubMed: 15181150]

Picciano JA, Ameen N, Grant BD, Bradbury NA. Rme-1 regulates the recycling of the cystic fibrosis transmembrane conductance regulator. Am J Physiol Cell Physiol. 2003; 285:C1009–18. [PubMed: 12839834]

Ramalho-Santos J, Schatten G, Moreno RD. Control of membrane fusion during spermiogenesis and the acrosome reaction. Biol Reprod. 2002; 67:1043–51. [PubMed: 12297516]

Ren M, Xu G, Zeng J, De Lemos-Chiarandini C, Adesnik M, Sabatini DD. Hydrolysis of GTP on rab11 is required for the direct delivery of transferrin from the pericentriolar recycling compartment to the cell surface but not from sorting endosomes. Proc Natl Acad Sci U S A. 1998; 95:6187–92. [PubMed: 9600939]

Riordan JR, Rommens JM, Kerem B, Alon N, Rozmahel R, Grzelczak Z, Zielenski J, Lok S, Plavsic N, Chou JL, et al. Identification of the cystic fibrosis gene: cloning and characterization of complementary DNA. Science. 1989; 245:1066–73. [PubMed: 2475911]

Roland JT, Kenworthy AK, Peranen J, Caplan S, Goldenring JR. Myosin Vb interacts with Rab8a on a tubular network containing EHD1 and EHD3. Mol Biol Cell. 2007; 18:2828–37. [PubMed: 17507647]

Rommens JM, Iannuzzi MC, Kerem B, Drumm ML, Melmer G, Dean M, Rozmahel R, Cole JL, Kennedy D, Hidaka N, et al. Identification of the cystic fibrosis gene: chromosome walking and jumping. Science. 1989; 245:1059–65. [PubMed: 2772657]

Sahlender DA, Roberts RC, Arden SD, Spudich G, Taylor MJ, Luzio JP, Kendrick-Jones J, Buss F. Optineurin links myosin VI to the Golgi complex and is involved in Golgi organization and exocytosis. J Cell Biol. 2005; 169:285–95. [PubMed: 15837803]

Seaman MN. Cargo-selective endosomal sorting for retrieval to the Golgi requires retromer. J Cell Biol. 2004; 165:111–22. [PubMed: 15078902]

Sonnichsen B, De Renzis S, Nielsen E, Rietdorf J, Zerial M. Distinct membrane domains on endosomes in the recycling pathway visualized by multicolor imaging of Rab4, Rab5, and Rab11. J Cell Biol. 2000; 149:901–14. [PubMed: 10811830]

Spudich G, Chibalina MV, Au JS, Arden SD, Buss F, Kendrick-Jones J. Myosin VI targeting to clathrin-coated structures and dimerization is mediated by binding to Disabled-2 and PtdIns(4,5)P(2). Nat Cell Biol. 2007; 9:176–83. [PubMed: 17187061]

Swiatecka-Urban A, Boyd C, Coutermarsh B, Karlson KH, Barnaby R, Aschenbrenner L, Langford GM, Hasson T, Stanton BA. Myosin VI regulates endocytosis of the cystic fibrosis transmembrane conductance regulator. J Biol Chem. 2004; 279:38025–31. [PubMed: 15247260]

Ullrich O, Reinsch S, Urbe S, Zerial M, Parton RG. Rab11 regulates recycling through the pericentriolar recycling endosome. J Cell Biol. 1996; 135:913–24. [PubMed: 8922376]

Wang H, Brautigan DL. A novel transmembrane Ser/Thr kinase complexes with protein phosphatase-1 and inhibitor-2. J Biol Chem. 2002; 277:49605–12. [PubMed: 12393858]

Wang H, Brautigan DL. Peptide Microarray Analysis of Substrate Specificity of the Transmembrane Ser/Thr Kinase KPI-2 Reveals Reactivity with Cystic Fibrosis Transmembrane Conductance Regulator and Phosphorylase. Mol Cell Proteomics. 2006; 5:2124–30. [PubMed: 16887929]

Warner CL, Stewart A, Luzio JP, Steel KP, Libby RT, Kendrick-Jones J, Buss F. Loss of myosin VI reduces secretion and the size of the Golgi in fibroblasts from Snell's waltzer mice. Embo J. 2003; 22:569–79. [PubMed: 12554657]

Wells AL, Lin AW, Chen LQ, Safer D, Cain SM, Hasson T, Carragher BO, Milligan RA, Sweeney HL. Myosin VI is an actin-based motor that moves backwards. Nature. 1999; 401:505–8. [PubMed: 10519557]

Yamashiro DJ, Tycko B, Fluss SR, Maxfield FR. Segregation of transferrin to a mildly acidic (pH 6.5) para-Golgi compartment in the recycling pathway. Cell. 1984; 37:789–800. [PubMed: 6204769]



Europe PMC Funders Author Manuscripts

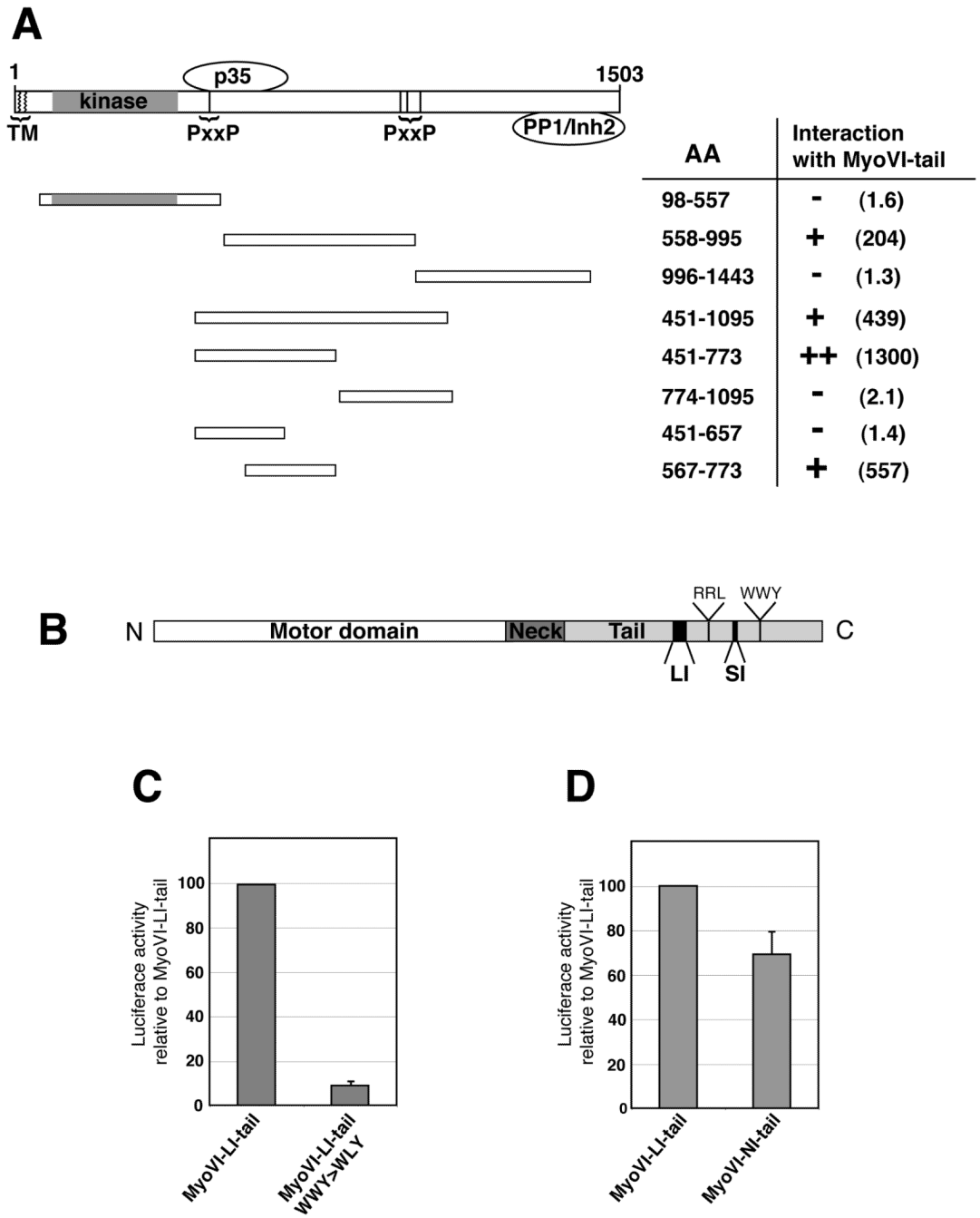


**Fig. 1.**

Mapping of the interaction domains in LMTK2 and myosin VI. The interaction between myosin VI and LMTK2, which was discovered in a yeast two-hybrid screen, was verified using a mammalian two-hybrid assay. (A) A cartoon showing the domain organisation of LMTK2. The kinase domain is highlighted in grey, two N-terminal putative transmembrane domains as zig-zag lines, PXXP motifs as black bars and the binding sites for p35 and PP1C/Inh2 are schematically shown. To map the binding site for myosin VI on LMTK2 CHO cells were co-transfected with myosin VI tail fused to Gal4 DNA-binding domain in pM, LMTK2 deletion fragments fused to the activating domain in pVP16 and two other plasmids, pG5luc and pRL-CMV, expressing inducible reporter and co-reporter

respectively. Relative luciferase activity was measured using Dual Luciferase Reporter Assay System kit (Promega). The deletion fragments used in this mammalian two-hybrid assay are depicted on the left and the corresponding amino acid (AA) numbers and the strength of the interaction (++, + or -) are shown, in brackets the actual luciferase activity relative to negative control is shown for a representative experiment. Fragment 567-773 is the minimal LMTK2 fragment that is still able to interact with myosin VI. (B) Schematic diagram of myosin VI domain organisation. LI - alternatively spliced 31 aa large insert, SI - 9 aa small insert, RRL - GIPC/opineurin binding motif, WWY - Dab2/LMTK2 binding motif. (C) Binding of myosin VI to LMTK2 requires the WWY motif. The mammalian two-hybrid assay was used to test binding of LMTK2 fragment 451-1095 against wild type myosin VI tail-LI or the tail containing a W1192L mutation (WWY->WLY). The graph shows mean±s.d. from three independent experiments. (D) LMTK2 binding to myosin VI does not require the large insert in the myosin VI tail. Binding of the LMTK2 fragment (451-1095) was tested against myosin VI tail containing the 31 aa insert (MyoVI-LI-tail) or the tail lacking the insert (Myo6-NI-tail). The data expressed as mean±s.d. from four independent experiments.

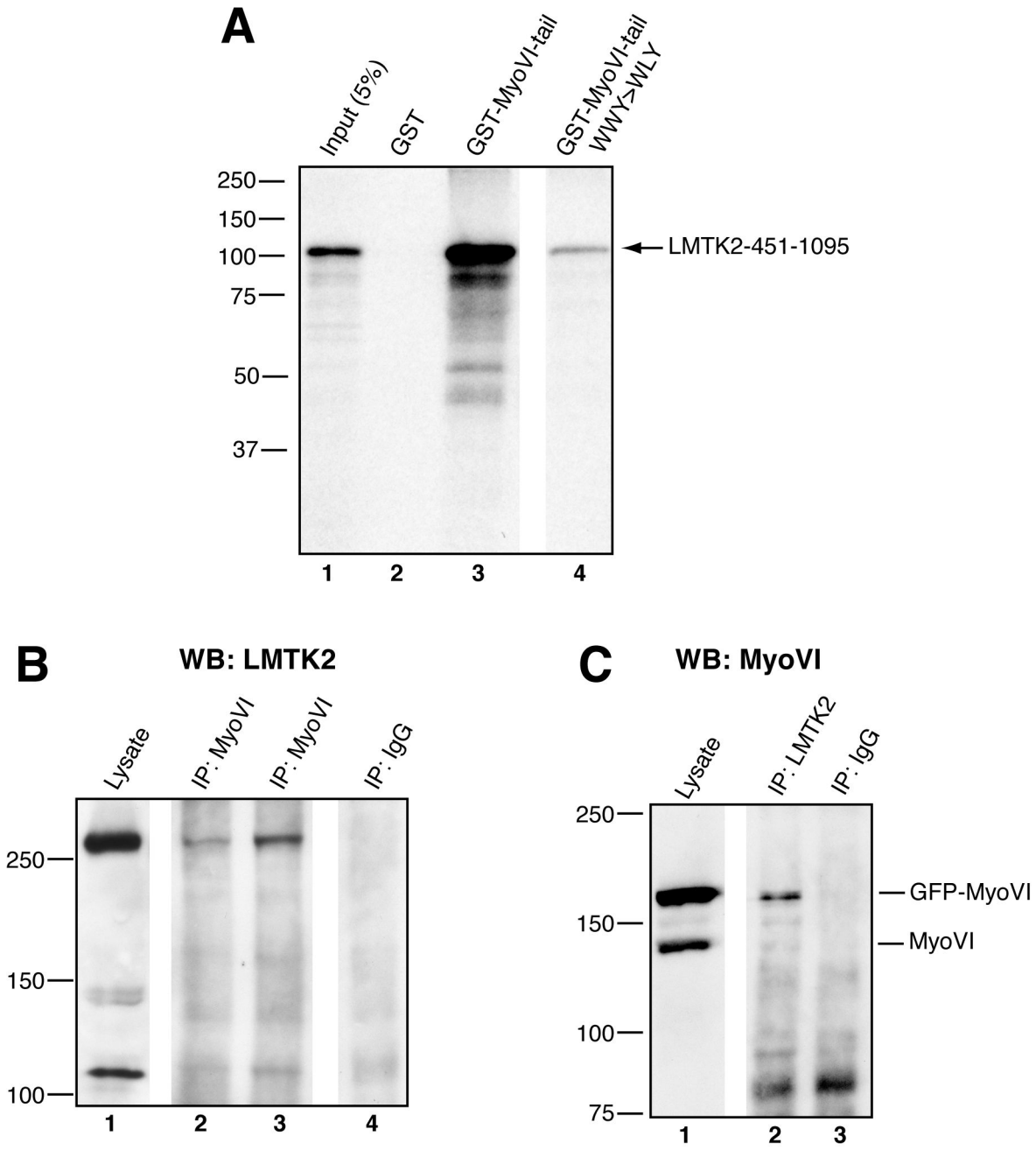


**Fig. 2.**

LMTK2 binds myosin VI *in vitro* and *in vivo*. (A) LMTK2 binds directly to purified myosin VI tail. A pull down was performed using *in vitro*-translated LMTK2 fragment and GST-myosin VI tail. [$^{35}$S]-labeled *in vitro*-translated LMTK2-451-1095 was incubated with 5 $\mu$g of either GST alone (2), GST-myosin VI tail (3) or GST-myosin VI tail with the W1192L mutation (WWY>WLY, lane 3). Lane 1 shows 5% of the input used for the pull downs. Mutation in the WWY motif within the myosin VI tail dramatically reduces LMTK2 binding. (B) (C) Co-immunoprecipitation of LMTK2 and myosin VI from HeLa cells. (B) HeLa cells, untransfected (lanes 1-2, 4) or transfected with GFP-myosin VI (lane 3), were lysed and myosin VI was immunoprecipitated using polyclonal antibodies to the myosin VI

tail (lanes 2-3). As a control immunoprecipitation was performed using non-immune rabbit IgG (lane 4). Lane 1 shows the whole cell lysate, which is equivalent to 5% of the input used for each immunoprecipitation. The immunoprecipitated protein complexes were blotted with antibodies to LMTK2. Please note the abnormal mobility of LMTK2 and its fragments on SDS-PAGE as described previously (Kawa et al., 2004). (C) Endogenous LMTK2 was immunoprecipitated from HeLa cells transfected with GFP-myosin VI and the immunoprecipitated complexes were blotted with anti-myosin VI tail antibodies. Lane 1 shows 5% of the whole cell lysate used for each immunoprecipitation and in lane 3 shows the negative control immunoprecipitation with non-immune rabbit IgG.

Europe PMC Funders Author Manuscripts

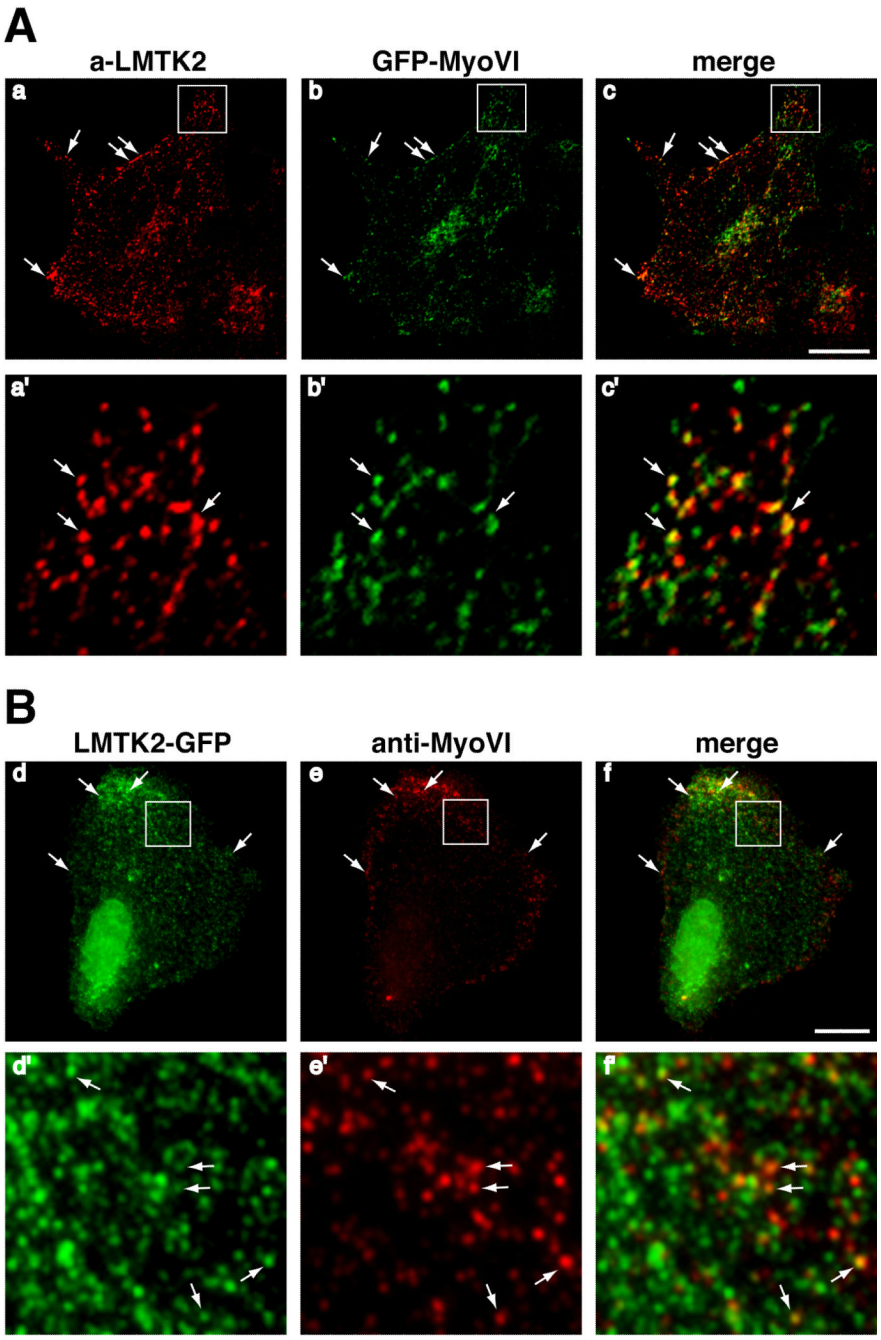


**Fig. 3.**

LMTK2 and myosin VI colocalise in cultured cells. (A) HeLa cells were co-transfected with untagged LMTK2 and GFP-tagged myosin VI and labelled with a polyclonal antibody to LMTK2 (a, a') and a monoclonal antibody to GFP (b, b'). Panels a, b and c are confocal z-stacks, panels a'-c' represent enlarged single confocal slices of boxed regions on panels a-c. (B) RPE cells were transfected with LMTK2-GFP and labelled with monoclonal antibody to GFP (d, d') and polyclonal antibody to myosin VI (e, e'). Wide field images are shown. Panels d'-f' represent enlarged boxed regions on panels d-f. Bar: 10 $\mu$m

Europe PMC Funders Author Manuscripts

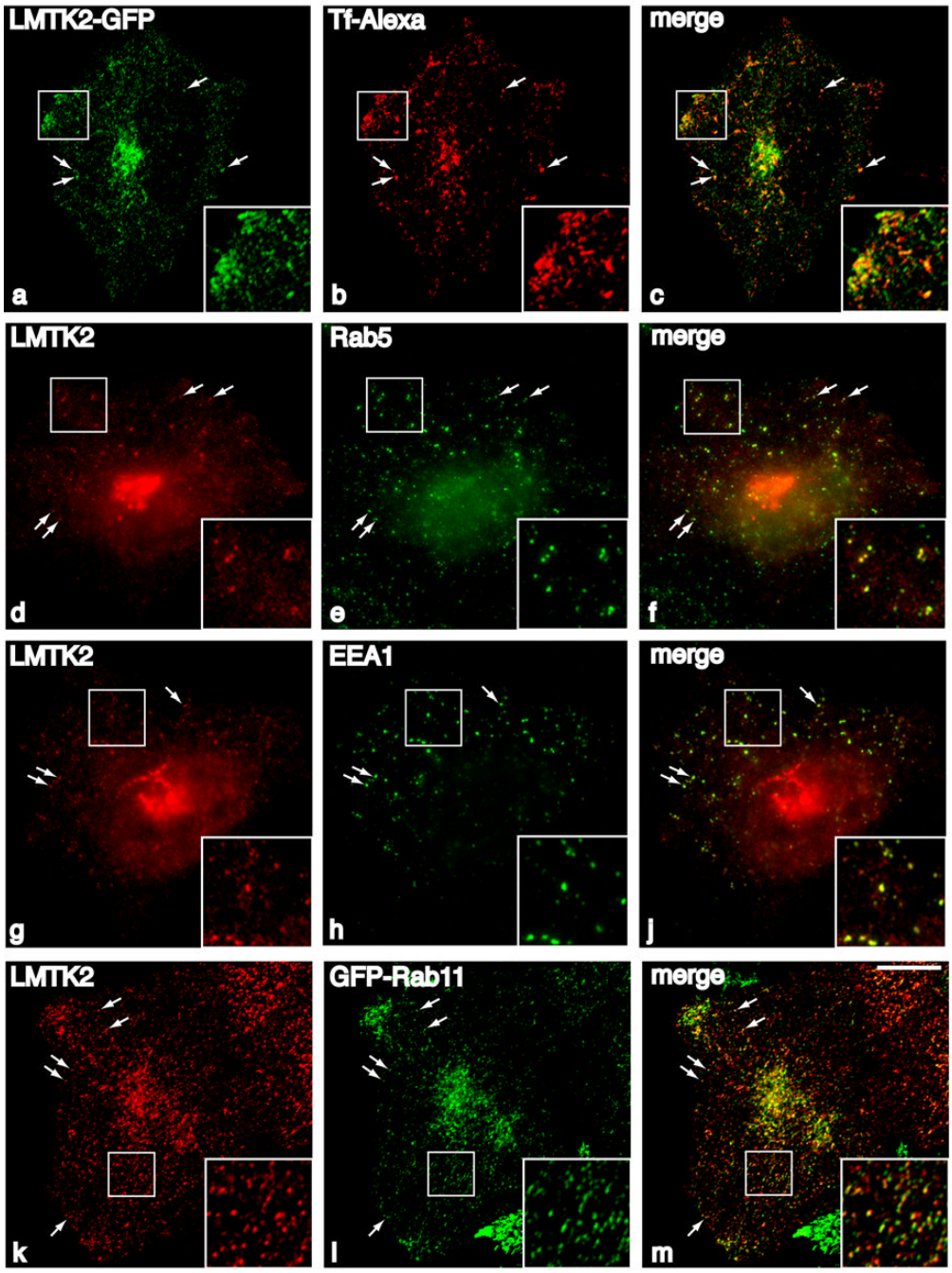


**Fig. 4.**

LMTK2 is present in the endocytic compartments. HeLa cells transfected with LMTK2-GFP were loaded with Tf-Alexa555 for 15 min, fixed and processed for immunofluorescence with anti-GFP antibody (a-c). HeLa cells transfected with untagged LMTK2 were immunolabelled for LMTK2 (d,g) and Rab5 (e) or EEA1 (h). HeLa cells stably expressing GFP-Rab11 were transfected with untagged LMTK2 and labelled with antibodies to LMTK2 and GFP (k-m). Merged images show LMTK2 colocalisation with the marker proteins in yellow. Single confocal slices (a-c, k-m) and wide field images (d-j) are shown. Insets represent enlarged images of the boxed regions. Bar: 10 $\mu$m.

Europe PMC Funders Author Manuscripts

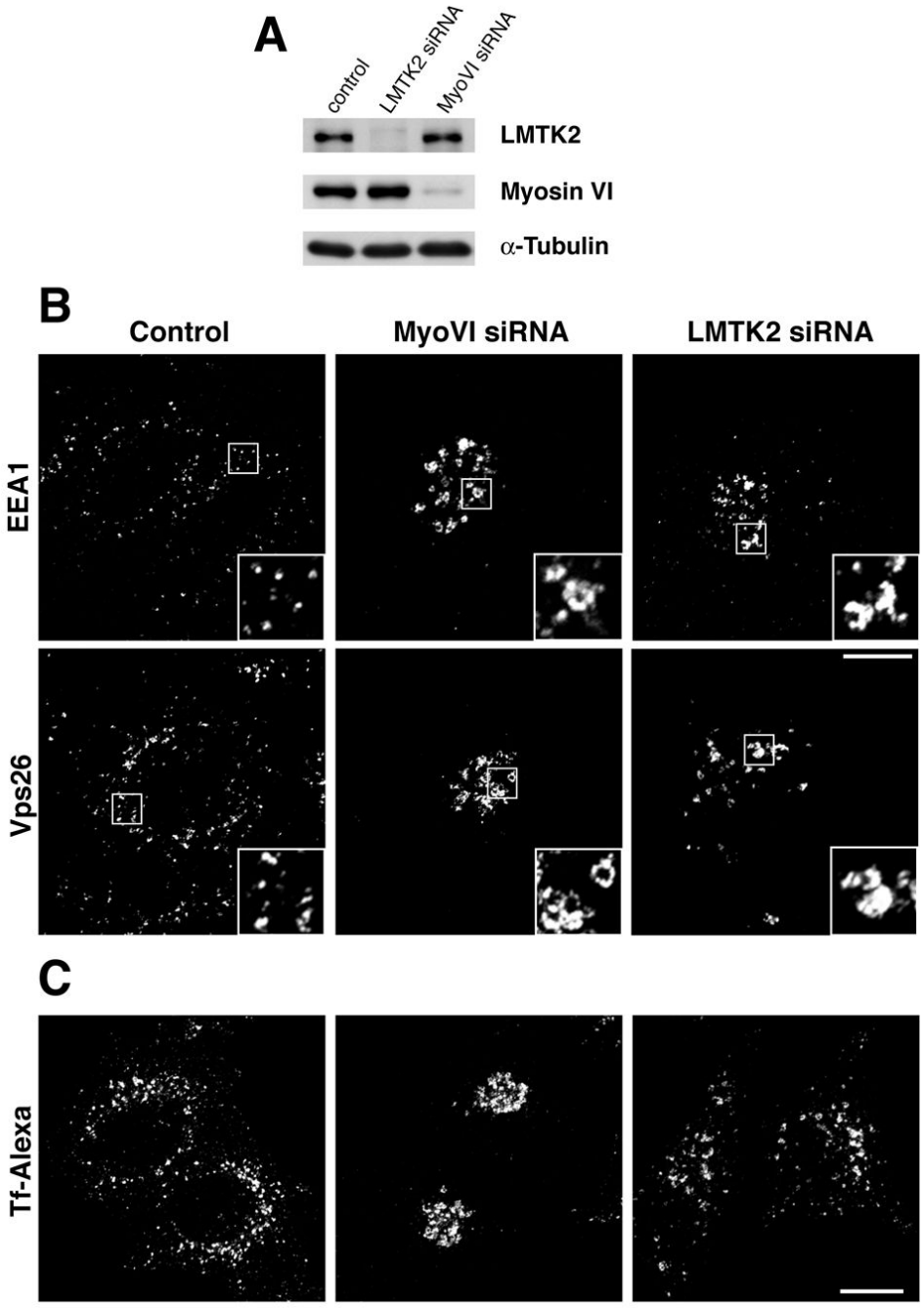


**Fig. 5.**

Depletion of myosin VI and LMTK2 changes the morphology and distribution of transferrin positive endosomes. HeLa cells were transfected twice with siRNA specific to myosin VI or LMTK2 or non-specific control siRNA. Two days after the second transfection the cells were harvested and (A) processed for Western blot with antibodies to LMTK2, myosin VI and alpha-tubulin. (B) In parallel experiments, the cells were immunolabelled for EEA1 and Vps26 or (C) were loaded with Tf-Alexa555 before fixation. Insets represent enlarged images of the boxed regions. All images shown are confocal z-projections. Bar: 10 $\mu$m

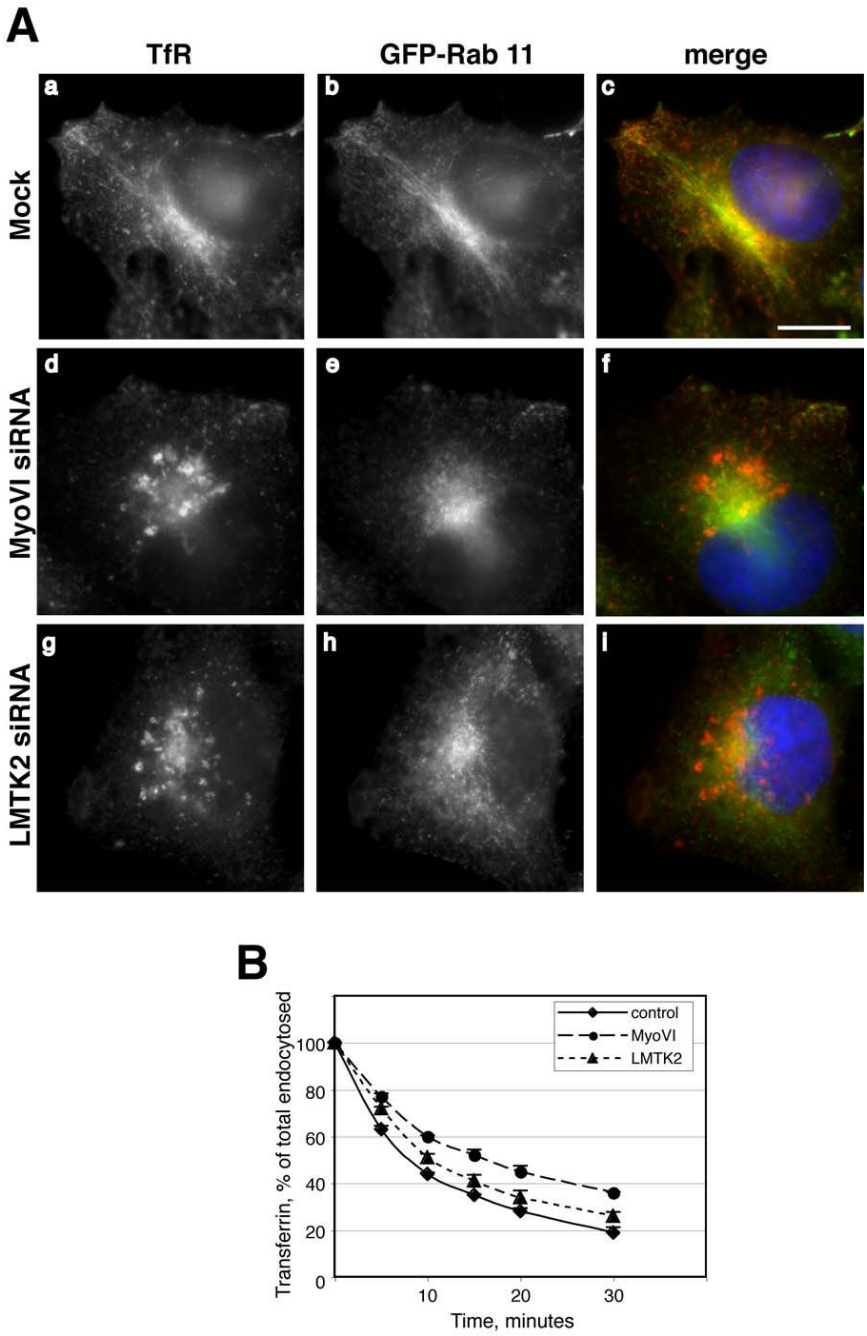


**Fig. 6.**

Depletion of myosin VI or LMTK2 inhibits delivery of transferrin receptor to the Rab11 positive perinuclear recycling compartment. (A) Hela cells stably expressing GFP-Rab11 were treated with siRNA to myosin VI or LMTK2 and processed for immunofluorescence with antibodies to the transferrin receptor (a, d, g) and to GFP (b, e, h) and labelled with DAPI to visualise nuclei. Merged images are shown in c, f and i. Bar: 10 $\mu$m. (B) HeLa cells transfected with myosin VI or LMTK2 siRNA were pulsed with Tf-Alexa647 at 37°C for 30 min, washed and incubated at 37°C in the presence of excess of unlabelled transferrin. The amount of Tf-Alexa647 per cell was determined by FACS analysis. The data is presented as mean±s.e. from three independent experiments, each performed in duplicate.

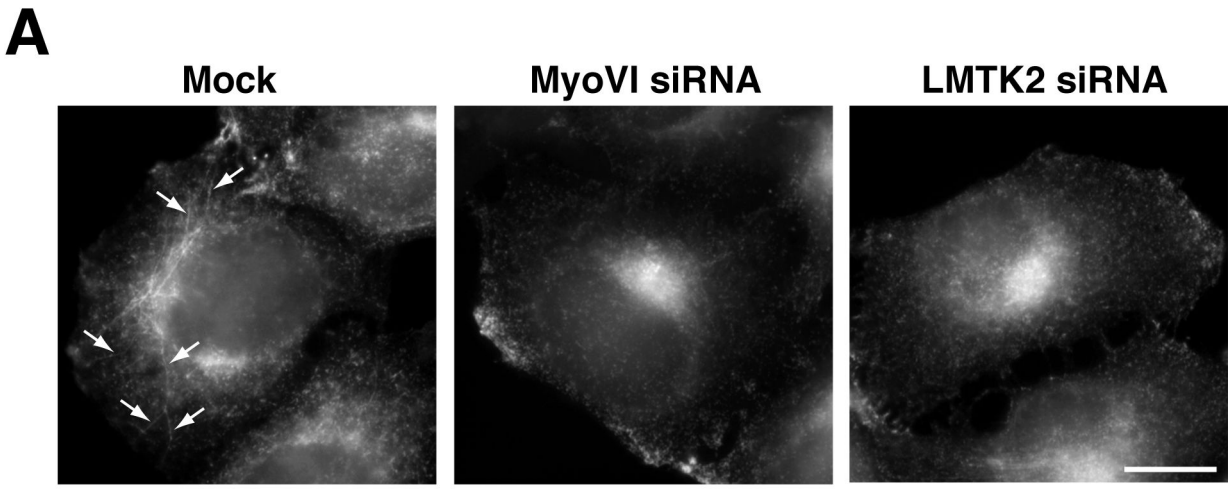


B

| | cells containing tubules (%) |
|---|---|
| Mock | 46±7 |
| MyoVI siRNA | 13±4 |
| LMTK2 siRNA | 26±8 |

**Fig. 7.**

Depletion of myosin VI and LMTK2 leads to reduction in Rab11-positive tubule formation. HeLa cells stably expressing GFP-Rab11 were treated with siRNAs to myosin VI or LMTK2 and processed for immunofluorescence with GFP antibodies. (A) A cell displaying a representative GFP-Rab11 distribution is shown for mock, myosin VI siRNA or LMTK2 siRNA treated cells. Whereas multiple tubules emanate from the juxtanuclear region in mock treated cells (arrows), an almost complete lack of tubules in both knockdowns was observed. In (B) a quantitation of the number of tubules in mock treated or KD cells is shown. At least 500 cells for the control and for each KD were counted and scored as either having or not having tubules. The results are expressed as percentage of cells containing tubules (mean±range from two independent experiments, each performed in triplicate). Bar: 10 $\mu$m

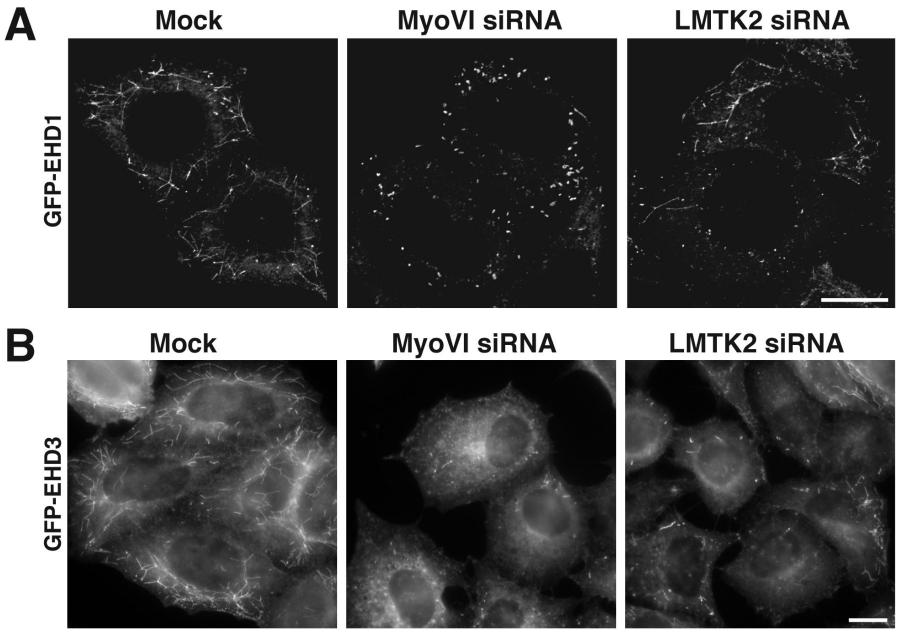


C

| | number of cells containing tubules (%) | | |
|---|---|---|---|
| | no tubules | few tubules | multiple tubules |
| Mock | 7±1.7 | 26±8 | 67±8 |
| MyoVI siRNA | 57±1 | 37±1.3 | 6±1.3 |
| LMTK2 siRNA | 19±2 | 62±5 | 19±2 |

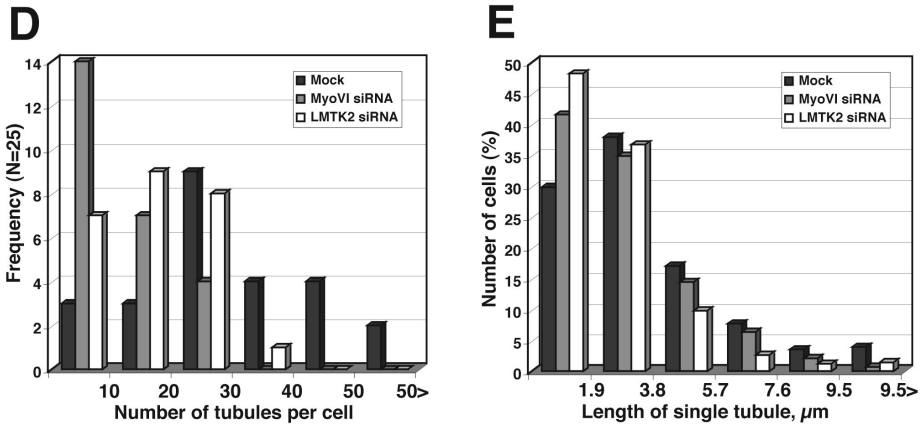


**Fig. 8.**

Depletion of myosin VI and LMTK2 leads to reduction in EHD1- and EHD3-positive tubule formation. Hela cells stably expressing GFP-EHD1 (A) or GFP-EHD3 (B-E) were treated with siRNA to myosin VI or LMTK2, fixed and mounted for immunofluorescence. Representative examples of GFP-EHD1 (A) or GFP-EHD3 (B) distribution are shown for each knockdown and control cells. (C) To quantify the number of EHD3 positive tubules in KD and control cells at least 200 randomly chosen cells were counted for each condition and scored as having either no, few (<15) or multiple (>15) tubules. The results are shown as percentage of cells for each category and are expressed as mean±s.d. from three independent experiments, each performed in triplicate. (D) and (E) The number of tubules was counted

and the length of individual tubules were measured in 25 cells for each knockdown. Cells without tubules were not taken into account in this quantitation. Branches were considered as separate tubules. The histograms depict the number of tubules per cell (D) and the length of individual tubules (E). In (A) confocal z-stacks and in (B) wide field images are shown. Bar: 10 $\mu$m



Europe PMC Funders Author Manuscripts

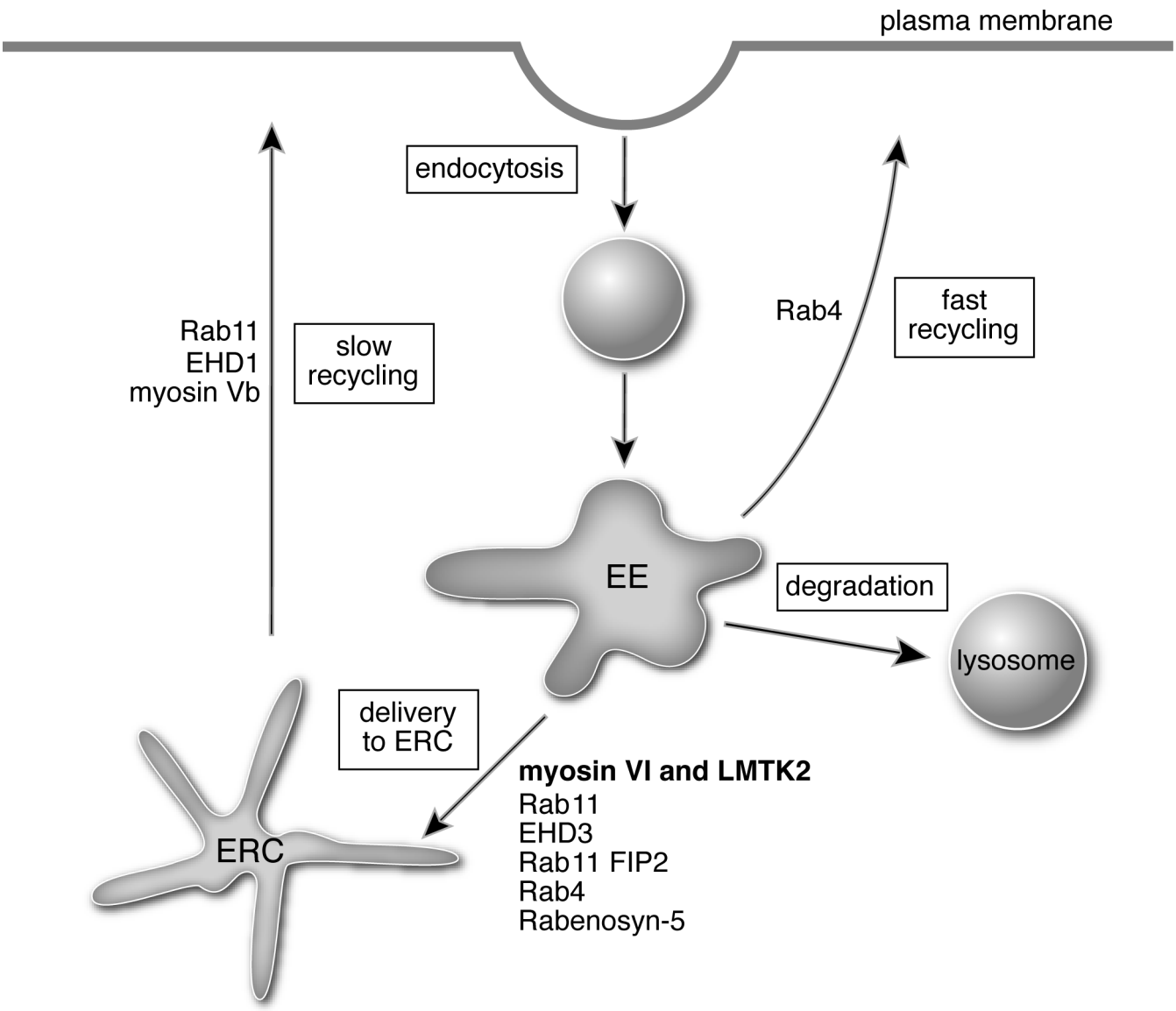


**Fig. 9.**

A cartoon illustrating the possible roles of LMTK2 and myosin VI in the delivery of cargo from the early endosome to the endocytic recycling compartment. After internalisation, endocytic vesicles are delivered to and fuse with the early endosome (EE), where proteins destined for degradation are sorted and transported to the lysosome. Proteins moving back to the cell surface can either take a fast recycling route directly from the EE or they take a slower route via the ERC. A number of proteins including Rab11, Rab1-FIP2, EHD3, Rab4 and Rabenosyn-5 have been shown to regulate trafficking between the EE and the ERC. Our results now add myosin VI, an actin motor protein and its binding partner LMTK2, a protein kinase, to this list of proteins required for delivery of cargo to the ERC. For the exit of receptors from the ERC the motor protein myosin Vb and also Rab11 and EHD1 are required.